J. Biochem. **135**, 117–128 (2004)
DOI: 10.1093/jb/mvh014

The Penta-EF-Hand Protein ALG-2 Interacts with a Region Containing PxY Repeats in Alix/AIP1, Which Is Required for the Subcellular Punctate Distribution of the Amino-Terminal Truncation Form of Alix/AIP1

Hideki Shibata, Keiko Yamada, Takako Mizuno, Chiharu Yorikawa, Hiroshi Takahashi, Hirokazu Satoh, Yasuyuki Kitaura[*] and Masatoshi Maki[†]

Laboratory of Molecular and Cellular Regulation, Department of Applied Molecular Biosciences, Graduate School of Bioagricultural Sciences, Nagoya University, Furo-cho, Chikusa-ku, Nagoya 464-8601

Received September 29, 2003; accepted November 20, 2003

ALG-2 is a Ca^{2+}-binding protein that belongs to the penta-EF-hand protein family and associates with several proteins, including annexin VII, annexin XI, and Alix/AIP1, in a Ca^{2+}-dependent manner. The yeast two-hybrid system and a biotin-tagged ALG-2 overlay assay were carried out to characterize the interaction between ALG-2 and Alix. The region corresponding to amino acid residues 794 to 827 in the carboxy-terminal proline-rich region of Alix was sufficient to confer the ability to interact directly with ALG-2. This region includes four-tandem PxY repeats. Alanine substitutions indicated that seven proline residues in this region, four in the PxY repeats, and four tyrosine residues in the PxY repeats are crucial for the binding affinity with ALG-2. Endogenous ALG-2 was co-immunoprecipitated in the presence of Ca^{2+} with FLAG-tagged Alix or FLAG-tagged AlixΔEBS, a deletion mutant lacking the endophilin binding consensus sequence, but not with FLAG-tagged AlixΔABS, another mutant lacking the region comprising amino acids 798–841, from the lysates of HEK293 cells transfected with each FLAG-tagged protein expression construct. FLAG-tagged ALG-2 overexpressed in HEK293 cells was also co-immunoprecipitated with Alix in a Ca^{2+}-dependent fashion, whereas FLAG-tagged ALG-$2^{E47A/E114A}$, a Ca^{2+}-binding deficient mutant of ALG-2, was not detected in the immunoprecipitates of Alix even in the presence of Ca^{2+}. Fluorescent microscopic analyses using the carboxy-terminal half of Alix fused with green fluorescent protein (GFP-AlixCT) revealed that endogenous ALG-2 in HeLa cells exhibits a dot-like pattern overlapping with exogenously expressed GFP-AlixCT, and the distribution of GFP-AlixCTΔABS is observed diffusely in the cytoplasm. These results indicate the requirement of ABS in Alix for the efficient accumulation of AlixCT and raise the possibility that ALG-2 participates in membrane trafficking through a Ca^{2+}-dependent interaction with Alix.

Key words: ALG-2, Alix/AIP1, calcium-binding protein, EF-hand, protein–protein interaction.

Abbreviations: GFP, green fluorescent protein; HA, hemagglutinin; HEK, human embryonic kidney; mAb, monoclonal antibody; PBS, phosphate buffered saline; PEF, penta-EF-hand; pAb, polyclonal antibody; PPII, polyproline II; PVDF, polyvinylidene difluoride; SH3, src homology 3; TBS, Tris-buffered saline.

Penta-EF-hand (PEF) proteins comprise a family of Ca^{2+}-binding proteins that have five repetitive EF-hand motifs, the PEF domain (*1*). The PEF domain was first revealed by X-ray crystallographic analysis of the Ca^{2+}-binding domain of the small subunit of calpain, an intracellular Ca^{2+}-dependent cysteine protease (*2*, *3*). The first EF-hand (EF1) motif is not consistent with the canonical EF-hand, in which a 12-residue interhelical sequence coordinates Ca^{2+} with pentagonal bipyramidal asymmetry. The EF1 of the calpain small subunit has an 11-residue loop sequence that can bind Ca^{2+} by coordinating with the carbonyl oxygen of the peptide bond in place of the side-chain oxygen of the canonical aspartic acid in the first Ca^{2+}-coordinating position (position X). In contrast, the fifth EF-hand (EF5) does not bind Ca^{2+} under physiological conditions due to a two amino acid insertion, but serves as dimerization domain. Re-evaluation of the primary sequence of multiple EF-hand proteins in mammals reveals the presence of a new family of members having the PEF domain (*4*) that are classified into two groups: Group I (ALG-2 and peflin) and Group II (calpain subfamily members, sorcin and grancalcin) (*1*). Most of these members have been shown to exist as non-covalent homodimers or heterodimers involving same group proteins under physiological conditions. ALG-2 forms either a homodimer or a heterodimer with peflin (*5*), which is essential for the stabilization of these PEF proteins in cells (*6*). The large and small subunits of the conventional

[*]The author is supported by Research Fellowships from the Japan Society for the Promotion of Science for Young Scientists.
[†]To whom correspondence should be addressed. Tel: +81-52-789-4088, Fax: +81-52-789-5542, E-mail: mmaki@agr.nagoya-u.ac.jp

calpains heterodimerize to form active proteases (*7*, *8*). Grancalcin also exists as a homodimer in solution and has been shown to interact with sorcin, but the functional significance of this complex is so far unknown (*9*). Most PEF proteins except for the calpain large subunit possess hydrophobic glycine/proline-rich regions at their N-termini, which are likely to play a role in the Ca^{2+}-dependent translocation of these proteins to biological membranes.

ALG-2 was originally identified during a screen for genes involved in apoptosis (*10*). The suppression of ALG-2 expression by an antisense transcript protects T-cell lines from cell death induced by several stimuli such as glucocorticoids, T-cell receptors and Fas triggering. Caspases are activated in ALG-2-depleted cells upon stimulation with these reagents, suggesting that ALG-2 exerts its function downstream or independent of protease activity in the apoptotic signaling pathway (*11*). Both immature thymocytes and mature T-cells from ALG-2-deficient mice retain their susceptibility to apoptotic stimuli (*12*). On the other hand, Group I genes analogous to ALG-2 have been found in lower eukaryotes (*13*, *14*). ALG-2 may, therefore, play additional roles in regulating fundamental cellular processes in response to Ca^{2+}-mobilization, including signal transduction, gene expression and membrane trafficking.

To gain insights into the function of ALG-2, searches for ALG-2-interacting proteins using yeast two-hybrid screening methods have been carried out by several groups (*15*–*17*). The first described murine target protein for ALG-2 was Alix or AIP1, named differently by two independent groups (*15*, *16*). The human homologue of this protein has been identified as Hp95, which is a homologue of *Xenopus* Xp95 (*18*, *19*). Human Alix consists of 868 amino acid residues and possesses a long proline-rich region in its C-terminus. Alix has been shown to be a positive regulator in apoptotic signaling and a negative regulator in cell transformation. Overexpression of the full-length protein in HeLa cells induces G1 arrest in confluent monolayer cultures, promotes detachment-induced apoptosis (anoikis), and reduces tumorigenicity (*19*, *20*). Furthermore, the overexpression of a truncated form of Alix retaining the C-terminal proline-rich region (AlixCT) protects transfected cells from death induced by the withdrawal of trophic factors (*16*). In contrast, previous studies on subcellular localization suggest that Alix is a novel membrane trafficking protein that is involved in modulating membrane shape, formation of the cytoplasmic compartment, and transport pathway. Overexpression of AlixCT in HEK293 cells leads to cytoplasmic vacuolization (*21*). This phenomenon appears to be enhanced by the co-expression of endophilin, which interacts directly with the proline-rich region of Alix (*21*) and regulates membrane shape, possibly through its lysophosphatidic acid transferase activity (*22*). We have recently shown that Alix associates with CHMP4b/Shax1, a human homologue of yeast Snf7/Vps32, which is involved in multivesicular body sorting (*23*). In HeLa cells overexpressing CHMP4b, Alix is recruited to putative endosomal compartments in which CHMP4b is distributed. The binding site for CHMP4b is located in the N-terminal half of Alix, whereas that for ALG-2 is thought to be in the C-terminal half, in which the last 150 amino acids are particularly rich in proline, tyrosine and glutamine, and which possesses several SH3 domain binding motifs (PxxP). In this study, we have narrowed the region in Alix that interacts with ALG-2 down to 33 amino acid residues containing four tandem PxY repeat sequences, and demonstrate the requirement of the ALG-2 binding site for the punctate distribution of AlixCT in mammalian cells.

EXPERIMENTAL PROCEDURES

Plasmid Constructions—The following plasmids were constructed for use in the yeast two-hybrid system. pGBT9-ALG-2 was described previously (*17*). pGAD424-Alix (680–848) was constructed by ligating the *Hin*cII/*Sma*I fragment of pCR2.1-TOPO-Alix (*23*) into the *Sma*I site of pGAD424 (Clontech). pACT2-Alix (680–868) was constructed by ligating the *Hin*cII/*Pvu*II fragment of pCR2.1-TOPO-Alix into the *Sma* I site of pACT2 (Clontech). pGAD424-Alix (680–868) was constructed by ligating the *Bgl*II fragment of pACT2-Alix (680–868) into the *Bgl*II site of pGAD424. The C-terminal and N-terminal deletion mutants of the proline-rich region of Alix were derived from pGAD424-Alix (680–848) and pGAD424-Alix (680–868), respectively, using Exonuclease III to create nested deletion mutants (Deletion Kit for Kilo-Sequencing, TAKARA, Osaka). For the C-terminal deletion mutants, pGAD424-Alix (680–848) was digested with *Pst*I and *Bam*HI, whereas for the N-terminal deletion mutants, pGAD424-Alix (680–868) was digested with *Pst*I and *Nhe*I. The deletion mutants were sequentially generated with Exonuclease III and Mung Bean Nuclease. pGAD424-Alix (680–823), pGAD424-Alix (680–834), and pGAD424-Alix (680–847) were digested with *Eco*RV, and the resultant smaller fragments were ligated with the *Eco*RV-digested larger fragment of pGAD424-Alix (796–868) to construct pGAD424-Alix (796–823), pGAD424-Alix (796–834), and pGAD424-Alix (796–847), respectively. pGAD424-Alix (680–847) was digested with *Eco*RV, and the resultant smaller fragment was ligated with the *Eco*RV-digested larger fragment of pGAD424-Alix (790–868) to construct pGAD424-Alix (790–847).

The following plasmids were constructed for use in mammalian cell transfections. pGFP-Alix and pFLAG-Alix, for the expression of GFP-fused and FLAG-tagged full-length human Alix, were constructed by ligating the *Eco*RI fragment of pCR2.1-TOPO-Alix into the *Eco*RI site of pEGFP-C3 (Clontech) and pCMV-Tag2C (Stratagene), respectively. To delete the cDNA fragment corresponding to Alix (amino acid residues 800–814) from the full-length human Alix cDNA, pUC119-Alix (680–848) was first constructed by ligating the *Hin*cII/*Sma*I fragment of pCR2.1-TOPO-Alix into the *Sma*I site of pUC119. Next, the forward oligonucleotide 5′-TCAGCTCCACCTCCACAGGCGCAAATGCCTATGCC-3′ and reverse oligonucleatide 5′-CATGGGCATAGGCATTTGCGCCTGTGGAGGTGGAGC-3′ were inserted between the *Bpu*1102I and *Nco*I sites of pUC119-Alix (680–848) to construct pUC119-Alix (680–848)$\Delta(PxY)_4$. Then, pCR2.1-TOPO-Alix$\Delta(PxY)_4$ was constructed by ligating the *Stu*I/*Sma*I fragment of pUC119-Alix (680–848)$\Delta(PxY)_4$ into the *Stu*I/*Sma*I site of pCR2.1-TOPO-Alix. Finally, pGFP-Alix$\Delta(PxY)_4$ and pFLAG-Alix$\Delta(PxY)_4$ were constructed by ligating the *Eco*RI frag-

Table 1. **Oligonucleotides used in the construction of Alix (794–827) with point mutations.**

Plasmid	Orientation	Sequence of 1st oligonucleotide[a]	Sequence of 2nd oligonucleotide
pGFP-Alix (794–827)	Forward	AGCTTCACCACCACAGGCGCAGGGACCACCATAT CCGACCTATCCAGGGTACCCAGGCTACTGCCA	GATGCCAATGCCCATGGGCTATAACCCATATGC GTACG
	Reverse	ATAGGTCGGATATGGTGGTCCCTGCGCCTGTGGT GGTGA	GATCCGTACGCATATGGGTTATAGCCCATGGGC ATTGGCATCTGGCAGTAGCCTGGGTACCCTGG
pGFP-P4A	Forward	AGCTTCACCACCACAGGCGCAGGGA*G*CACCATAT *G*CGACCTAT*G*CAGG*G*TA*CG*CAGGCTACTGCCA	GATGCCAATGCCCATGGGCTATAACCCATATGC GTACG
	Reverse	ATAGGTCG*C*ATATGGTG*C*TCCCTGCGCCTGTGGT GGTGA	GATCCGTACGCATATGGGTTATAGCCCATGGGC ATTGGCATCTGGCAGTAGCCTG*C*GTACCCTG*C*
pGFP-Y4A	Forward	AGCTTCACCACCACAGGCGCAGGGACCACC*AGCT* CCGACC*GC*TCCAGGA*GCT*CCAGGA*GCC*TGCCA	GATGCCAATGCCCATGGGCTATAACCCATATGC GTACG
	Reverse	A*GC*GGTCGGA*GC*TGGTGGTCCCTGCGCCTGTGGT GGTGA	GATCCGTACGCATATGGGTTATAGCCCATGGGC ATTGGCATCTGGCA*GGC*TCCTGGA*GC*TCCTGG
pGFP-Y4F	Forward	AGCTTCACCACCACAGGCGCAGGGACCACCAT*T*T CCGACCTT*C*CCAGGGT*T*TCCCGGGTT*C*TGCCA	GATGCCAATGCCCATGGGCTATAACCCATATGC GTACG
	Reverse	*GA*AGGTCGGA*A*ATGGTGGTCCCTGCGCCTGTGGT GGTGA	GATCCGTACGCATATGGGTTATAGCCCATGGGC ATTGGCATCTGGCAG*A*ACCCGGGA*A*ACCCTGG
pGFP-P3A	Forward	AGCTTCACCACCACAGGCGCAGGGACCACCATAT CCGACCTATCCAGGGTACCCAGGCTACTGCCA	GATG*G*CAATG*G*CCATGGGCTATAAC*G*CATATGC GTACG
	Reverse	ATAGGTCGGATATGGTGGTCCCTGCGCCTGTGGT GGTGA	GATCCGTACGCATATG*C*GTTATAGCCCATGG*C*C ATTG*C*CATCTGGCAGTAGCCTGGGTACCCTGG
pGFP-Y3A	Forward	AGCTTCACCACCACAGGCGCAGGGACCACCATAT CCGACCTATCCAGGGTACCCAGGCTACTGCCA	GATGCCAATGCCCATGGGC*GC*TAACCCA*GC*TGC G*GCC*G
	Reverse	ATAGGTCGGATATGGTGGTCCCTGCGCCTGTGGT GGTGA	GATC*CGGC*CGCA*GC*TGGGTTA*GC*GCCCATGGG CATTGGCATCTGGCAGTAGCCTGGGTACCCTGG

[a]All sequences are depicted in the 5′ to 3′ direction. Nucleotides corresponding to the human Alix sequence are underlined. Nucleotides in italics indicate codon substitution sites.

ment of pCR2.1-TOPO-AlixΔ$(PxY)_4$ into the *Eco*RI site of pEGFP-C3 and pCMV-Tag2C, respectively. To delete the cDNA fragment corresponding to Alix (amino acid residues 798–841), the forward oligonucleotide 5′-TCAGCACCTGGACAGGCTCCATACCC-3′ and reverse oligonucleotide 5′-GGGTATGGAGCCTGTCCAGGTGC-3′ were inserted between between the *Bpu*1102I and *Sma*I sites of pUC119-Alix (680–848). The resultant plasmid was designated pUC119-Alix (680–848)ΔABS. Then, pCR2.1-TOPO-AlixΔABS was constructed by ligating the *Stu*I/*Sma*I fragment of pUC119-Alix (680–848)ΔABS into the *Stu*I/*Sma*I site of pCR2.1-TOPO-Alix. Finally, pGFP-AlixΔABS and pFLAG-AlixΔABS were constructed by ligating the *Eco*RI fragment of pCR2.1-TOPO-AlixΔABS into the *Eco*RI site of pEGFP-C3 and pCMV-Tag2C, respectively. pFLAG-AlixΔEBS, for the expression of a FLAG-tagged deletion mutant of Alix lacking the region comprising amino acid residues 757–764, was constructed in a pFLAG-Alix plasmid using the PCR-based Quickchange Site-Directed Mutagenesis Kit (Stratagene). The primers used for deletion were as follows, 5′-CCAGCCCCCAGCCATTCCAGCAAATCGAGCT-3′ and 5′-AGCTCGATTTGCTGGAATGGCTGGGGGCTGG-3′. pGFP-Alix (790–847) was constructed by ligating the *Bam*HI/*Sma*I fragment of pGAD424-Alix (790–847) into the *Bgl*II/*Sma*I site of pEGFP-C2. pGFP-Alix (794–827) and mutant derivatives were constructed by inserting two pairs of double-stranded oligonucleotides (Table 1) into the *Hin*dIII/*Bam*HI site of pEGFP-C1. The cDNA fragments corresponding to AlixCT (amino acid residues 458–868), AlixCT lacking the endophilin-binding site (amino acid residues 757–764) or AlixCT lacking the ALG-2-binding site (amino acid residues 798–841) were isolated by PCR with the primers, 5′-TGGATGAAGAAGAAGCAACCG-3′ and 5′-CAGAGCGTAGAGTTTAGTACAC-3′, and pFLAG-Alix, pFLAG-AlixΔEBS or pFLAG-AlixΔABS as templates, respectively. The PCR products were cloned into pCR2.1-TOPO to generate pCR2.1-TOPO-AlixCT, pCR2.1-TOPO-AlixCTΔEBS and pCR2.1-TOPO-AlixCTΔABS. pGFP-AlixCT, pGFP-AlixCTΔEBS and pGFP-AlixCTΔABS were constructed by ligating the *Eco*RI fragments of pCR2.1-TOPO-AlixCT, pCR2.1-TOPO-AlixCTΔEBS and pCR2.1-TOPO-AlixCTΔABS into the *Eco*RI site of pEGFP-C3, respectively. Screening to isolate the cDNA fragment of endophilin I (amino acid residues 22–352) was performed using a HeLa cell cDNA library in pGAD-GH (Clontech) with a fragment of Alix (amino acid residues 680–868) fused to the Gal4 DNA binding domain as bait in the yeast two-hybrid screening. pTicHA-b-endophilin I (22–352) was constructed by ligating the *Bam*HI/*Kpn*I fragment of pGAD-GH-endophilin I (22–352) into the *Bam*HI/*Kpn*I site of pTicHA-b (*24*). pHA-endophilin I was constructed by ligating the *Hin*dIII fragment of pTicHA-b-endophilin I (22–352) into the *Hin*dIII site of pcDNA3 (Invitrogen). pFLAG-ALG-2 was described previously (*5*). The point mutations at the first and third EF-hands of ALG-2 were introduced by the Quickchange Site-Directed Mutagenesis Kit using a combination of following primers, E47A, 5′-ATATCAGACACCGCGCTTCAGCAAGCT-3′ and 5′-AGCTTGAAGCGCGGTGTCTGATAT-3′; E114A 5′-ATCGATAAGAACGCGCTGAAGCAGGCC-3′ and 5′-GGCCTGCTTCAGCGCGTTCTTATCGAT-3′.

Yeast Two-Hybrid System—Different combinations of yeast expression plasmids were co-transformed into yeast AH109 cells (Clontech) and transformants were plated on synthetic complete plates lacking leucine and tryptophan (SD/-Leu/-Trp). At least five independent colonies on each SD/-Leu/-Trp plate were streaked onto synthetic complete plates lacking leucine, tryptophan, histidine and adenine, but supplemented with 5 mM 3-amino-

1,2,4-triazole (SD/-Leu/-Trp/-His/-Ade), and examined for growth (histidine and adenine prototrophy) at 30°C.

Antibodies—The following antibodies were purchased: anti-GFP polyclonal antibody (pAb) (ab290, Abcam), anti-GFP monoclonal antibody (mAb) (B-2, Santa Cruz Biotechnology, Santa Cruz), anti-FLAG mAb (M2, SIGMA) and anti-HA mAb (3F10, Roche). Rabbit anti-ALG-2 pAb was prepared as described previously (*25*) and affinity-purified using recombinant human ALG-2 (*5*). Peroxidase-conjugated goat anti-mouse and anti-rabbit IgG were purchased from Jackson Immuno Research Laboratories, Inc. Peroxidase-conjugated goat anti-rat IgG was from Santa Cruz. Cy3-labelled goat anti-rabbit and anti-mouse IgG used for indirect immunofluorescence analyses were purchased from Amersham Pharmacia.

Cell Culture—HEK293 and HeLa cells were cultured in Dulbecco's modified Eagle's medium supplemented with 10% heat-inactivated fetal bovine serum, 100 unit/ml penicillin and 100 μg/ml streptomycin at 37°C under humidified air containing 5% CO_2.

Bio-ALG-2 Overlay Assay—Biotin-tagged ALG-2 (bio-ALG-2) was purified as described previously (*17*). One day after HEK293 cells (1×10^6) were seeded, they were transfected with expression plasmid DNAs by the conventional calcium phosphate precipitation method. After 24 h, the cells were washed with PBS (137 mM NaCl, 2.7 mM KCl, 8 mM Na_2HPO_4, 1.5 mM KH_2PO_4, pH 7.3) and lysed in SDS-PAGE sample buffer. Proteins were resolved by SDS-PAGE and then transferred to PVDF membranes (Immobilon-P, Millipore). Nonspecific binding of bio-ALG-2 to the blotted membranes was blocked by immersion of the blots in TBS (20 mM Tris-HCl, pH 7.5, 150 mM NaCl)/0.1% Tween 20/1% gelatin/0.02% sodium azide at 37°C for 1 h. After washing with TBS/0.1% Tween 20/0.1 mM $CaCl_2$, the blots were incubated with 20 ng/ml bio-ALG-2 in TBS/0.1% Tween 20/0.1 mM $CaCl_2$/0.1% gelatin at 4°C overnight. After washing twice with TBS/0.1% Tween 20/0.1 mM $CaCl_2$ for 5 min each time, the blots were incubated with 1 μg/ml horseradish peroxidase-conjugated avidin (EY Laboratories) in TBS/0.1% Tween 20/0.1 mM $CaCl_2$/0.1% gelatin at 37°C for 15 min. After washing twice with TBS/0.1% Tween 20/0.1 mM $CaCl_2$ and three times with TBS/0.1 mM $CaCl_2$ for 5 min each time, bound bio-ALG-2 was detected by developing the blots in 0.1 M Tris-HCl, pH 7.5, containing 0.1 mM $CaCl_2$, 40 mg/ml diaminobenzidine, 80 mg/ml $NiCl_2$ and 0.01% H_2O_2.

Co-Immunoprecipitation Assay—One day after HEK293 cells (3×10^6) were seeded, they were transfected with expression plasmid DNAs by the conventional calcium phosphate precipitation method. After 24 h, the cells were washed with PBS and lysed in lysis buffer (20 mM HEPES-NaOH, pH 7.4, 0.2% Nonidet P-40, 142.5 mM KCl, 1.5 mM $MgCl_2$, 0.1 mM pefabloc, 25 μg/ml leupeptin, 1 μM E-64 and 1 μM pepstatin) containing 10 μM $CaCl_2$ or 2 mM EGTA. Supernatants obtained by centrifugation at 10,000 ×*g* were incubated with appropriate antibodies at 4°C for 3 h, then Dynabeads Protein G (Dynal Biotech) were added and the reaction was continued overnight. After washing the beads with the same buffer without protease inhibitors three times, the bound proteins were resolved by SDS-PAGE and then subjected to immunoblotting using appropriate antibodies. The immunoreactive bands were visualized by the chemiluminescent method using Super Signal West Pico Chemiluminescent Substrate (Pierce).

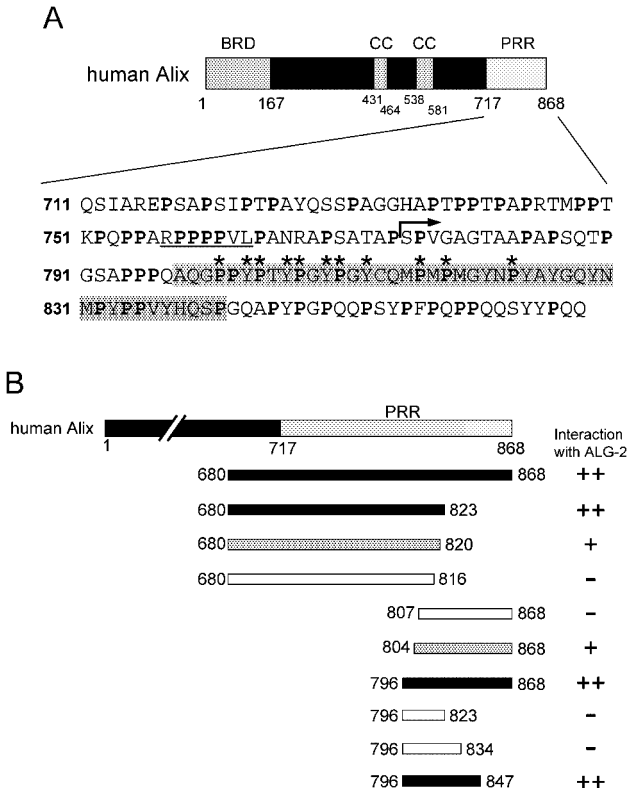

Fig. 1. **Identification of the ALG-2-interacting region in Alix using the yeast two-hybrid system.** A schematic structure of Alix is represented at the top. 'PRR' indicates a proline-rich region. (A) Sequence alignment of the proline-rich region in Alix. 'BRD' and 'CC' indicate a Bro1-rhophilin-like domain and coiled-coil region, respectively. The sequence of the proline-rich region in Alix is shown underneath. Proline residues are in bold. Clone 67 isolated in the two-hybrid screening was fused to the Gal4 activation domain at the position indicated by the arrow. The underlined region contains the endophilin-binding consensus sequence. The shaded region shows the ALG-2-binding site (ABS) in Alix identified in this work. Asterisks indicate critical residues for the recognition of Alix by ALG-2. (B) Specificity of the interaction of ALG-2 with deletion mutants of Alix. The numbers denote the amino acid positions of each mutant. The interaction between each mutant fused to the GAL4 transcription activation domain and ALG-2 fused to the GAL4 DNA-binding domain in transfected yeast AH109 cells was assessed by growth on SD/-Leu/-Trp/-His/-Ade. '++' and '+' indicate growth within 4 and 6 days from initiation of the assay, respectively. '–' indicates no growth within 6 days.

Immunofluorescence Microscopy—One day after HeLa cells (5×10^3) were seeded onto cover slips, they were transfected with expression plasmid DNAs using FuGENE6 according to the manufacturer's instructions (Roche). After 24 h, the cells were fixed in 4% paraformaldehyde/PBS and permeabilized in 0.1% Triton X-100/PBS. After blocking with 0.1% gelatin/PBS, the cells were incubated with the relevant antibody either at 4°C overnight or at room temperature for 1 h. The cells were washed with 0.01% Triton X-100/PBS, and the primary antibody reactive signal was visualized by subsequent incubation with the appropriate secondary antibody con-

jugated with Cy3. After washing with PBS, cells were mounted with anti-fading solution (25 mM Tris-HCl, pH 8.7, 10% polyvinyl alcohol, 5% glycerol, 2.5% 1,4-diazobicyclo (2,2,2)-octane). The fluorescences of GFP and Cy3 were analyzed with a confocal laser-scanning microscope, LSM5 PASCAL (Zeiss).

RESULTS

Mapping the ALG-2 Binding Region of Alix in the Yeast Two-Hybrid System—The full-length ALG-2 was used as bait in a yeast two-hybrid screen of a HeLa cell cDNA library as reported previously (*17*). One positive clone, clone 67, contained the open reading frame of amino acids 775 to 868 of human Alix (Fig. 1A). To delineate the region of Alix recognized by ALG-2, expression plasmids encoding a series of Alix cDNA deletion mutants fused to a GAL4 transcription activation domain were constructed. As shown in Fig. 1B, the yeast cells co-transformed with both fusion constructs for the carboxyl-terminal region of Alix (a.a. 680–868) and the full length ALG-2 were prototrophic for histidine and adenine. No obvious change in the interaction with ALG-2 was detected when the carboxyl-terminal 45 amino acids of Alix were additionally deleted. However, the Alix (a.a. 680–820) mutants showed less robust growth on histidine- and adenine-deficient medium, suggesting a decreased ability to interact with ALG-2. The interaction with ALG-2 was completely absent in Alix (a.a. 680–816), which retained four tandemly arranged PxY repeats (see Fig. 1A), demonstrating that this characteristic sequence is not sufficient to mediate the interaction in this system. The region between amino acids 817 and 823 is necessary for the full binding activity of Alix with ALG-2, whereas the region between amino acids 817 and 820 (MPMG) is crucial for the interaction. Similarly, a decrease in the interaction with ALG-2 was noted between Alix (a.a. 796–868) and Alix (a.a. 804–868), demonstrating a requirement for the region between 796 and 803, including the first PxY motif. An additional deletion mutant, Alix (a.a. 807–868), which lacks the first and second PxY motifs, did not interact with ALG-2, suggesting that four repeats of the PxY sequence are necessary for the interaction of ALG-2 with Alix.

The above data indicate that the region between amino acids 796 and 823 of Alix is necessary for the interaction with ALG-2. We tested whether this Alix domain is also sufficient for this interaction. Alix (a.a. 796–823) and Alix (a.a. 796–834) constructs failed to interact with ALG-2 in this assay. In contrast, Alix (a.a. 796–847) exhibited interaction comparable to that of Alix (a.a. 680–868). This analysis, therefore, identifies a 13-amino acid region of Alix, encompassing residues 835–847, that is required for full binding activity in the yeast two-hybrid system.

ALG-2 Binds Directly to Alix In Vitro—Previous investigations using co-immunoprecipitation and pull-down assays disclosed that ALG-2 associates with Alix in a Ca^{2+}-dependent fashion (*15*, *16*). The interaction of ALG-2 with Alix in various experimental assays containing our yeast two-hybrid system raises the question of whether ALG-2 binds directly to Alix or whether it might associate indirectly with Alix *via* binding to other

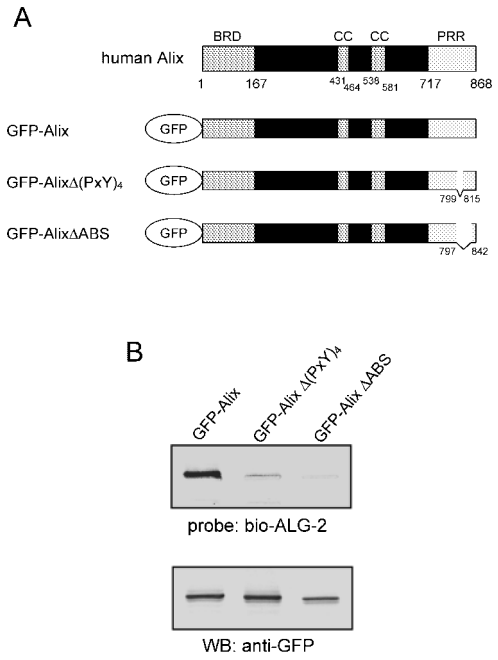

Fig. 2. **Expression and ligand overlay assay of deletion mutants of Alix.** (A) Schematic representation of Alix deletion constructs. 'BRD', 'CC' and 'PRR' indicate a Bro1-rhophilin-like domain, coiled-coil and proline-rich region, respectively. The numbers denote the amino acid positions of each mutant. (B) HEK293 cells were transiently transfected with pGFP-Alix or pGFP-Alix deletion constructs. Cell lysates were subjected to SDS-PAGE and transferred to PVDF membranes. The membrane was then probed either with biotin-tagged ALG-2 (bio-ALG-2) in the presence of Ca^{2+} (upper panel) or with a monoclonal anti-GFP antibody (lower panel).

unknown endogenous components. To test the ability of ALG-2 to bind directly to Alix, we carried out an *in vitro* "overlay" binding assay. The recombinant biotin-tagged ALG-2 proteins (bio-ALG-2) were bacterially expressed and purified (*17*) and then used as a probe. The GFP-fused Alix (GFP-Alix) or Alix-deletion mutants transiently expressed in HEK293 cells were separated by SDS-PAGE and then analyzed by overlay assay in the presence of Ca^{2+} or Western blotting (Fig. 2). A signal of bio-ALG-2 binding was observed with GFP-Alix (Fig. 2B, lane 1). Since no signal was detected in this system in the absence of Ca^{2+} (data not shown), bio-ALG-2 binds directly to GFP-Alix in a Ca^{2+}-dependent manner. The signal was significantly reduced by the deletion of a 15-amino acid region [AlixΔ$(PxY)_4$], corresponding to the entire PxY repeat, and became barely visible with GFP-fused Alix that lacked amino acids 798–841, which we named GFP-AlixΔABS (ALG-2 binding sequence) (Fig. 2B, lanes 2 and 3).

Characterization of Amino Acids in Alix That Govern the Interaction with ALG-2—To guide studies on amino acids that are crucial for the direct interaction of ALG-2, we first identified the minimal region in Alix that binds directly to ALG-2. As expected from the two-hybrid data, the interaction of bio-ALG-2 with GFP-Alix (a.a. 790–847) was observed (Fig. 3B, lane 2), whereas no interaction was detected between bio-ALG-2 and GFP (Fig. 3B, lane 1). In addition, a shorter region in Alix, correspond-

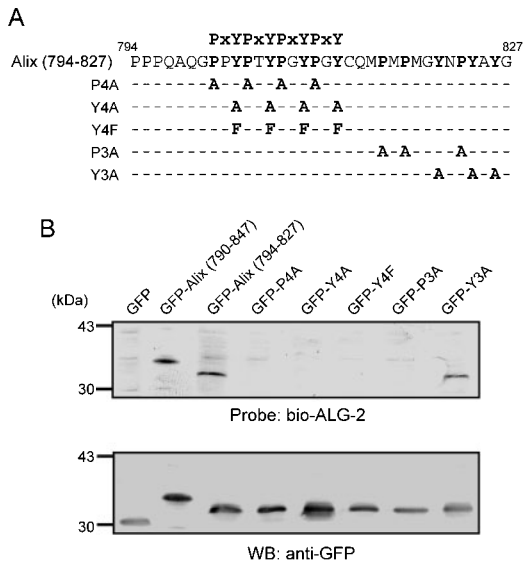

Fig. 3. **Expression and ligand overlay assay of point mutants of Alix.** (A) Positions of point mutations. A partial amino acid sequence of Alix (a.a. 794–827) is shown with inserted point mutations indicated in bold. Mutated residues in each derivative are shown in bold. The characteristic four-tandem PxY repeat sequence is shown. (B) HEK293 cells were transiently transfected with pGFP, pGFP-Alix (790–847), pGFP-Alix (794–827) or pGFP-Alix (794–827) point mutation constructs. Cell lysates were subjected to SDS-PAGE and transferred to PVDF membranes. The membrane was then probed either with biotin-tagged ALG-2 (bio-ALG-2) in the presence of Ca^{2+} (upper panel) or with a monoclonal anti-GFP antibody (lower panel).

ing to amino acids 794–827, was recognized by bio-ALG-2 (Fig. 3B, lane 3), suggesting that this region in Alix (Fig. 3A) is responsible for the direct interaction with ALG-2. Next, we introduced several point mutations into GFP-Alix (794–827) and analyzed their effects on ALG-2 binding. We chose proline and tyrosine residues in the four-tandem PxY repeats, as well as those located on its carboxyl terminal side of Alix (794–827), to introduce mutations. These mutants were expressed as GFP fusion proteins in HEK293 cells and the expressed proteins were analyzed by SDS-PAGE and overlay assay (Fig. 3B, lanes 4–8). The signal observed with GFP-Alix (794–827) disappeared with P4A, Y4A, Y4F, and P3A mutations, whereas the Y3A mutation had no effect on complex formation with ALG-2. These results indicate that proline residues in Alix (794–827) and tyrosine residues in the PxY repeats are crucial for the interaction with ALG-2.

ABS in Alix as a Required Region for the Interaction with ALG-2 in Mammalian Cells—To verify the region in Alix responsible for ALG-2 binding as revealed in the bio-ALG-2 overlay experiments, HEK293 cells were transfected with expression plasmids encoding different forms of Alix tagged with the FLAG epitope (Fig. 4A). Empty vector was used as a negative control. The cell lysates were subjected to immunoprecipitation with anti-FLAG mAb in the presence or absence of Ca^{2+} and the immunoprecipitates were probed with anti-ALG-2 pAb (*25*). In all co-immunoprecipitation experiments (see Figs. 4B and 6A), we observed that most endogenous or epitope-tagged ALG-2 was recovered in the soluble fraction in lysis buffer in the absence of Ca^{2+}, whereas, in the presence of Ca^{2+}, about half of both proteins were in the insoluble fractions. As shown in Fig. 4B, soluble ALG-2 was co-precipitated with FLAG-Alix by anti-FLAG mAb in the presence of Ca^{2+} (lane 1), but not in the presence of the Ca^{2+} chelator EGTA (lane 2). No ALG-2 was detected in precipitates of FLAG-tagged Alix that lacked the ABS, FLAG-AlixΔABS, in either the presence or absence of Ca^{2+} (lanes 3 and 4). This suggests that the ABS in Alix is required for the Ca^{2+}-dependent interaction between ALG-2 and Alix in mammalian cells, and is consistent with the results of the bio-ALG-2 overlay assay (Fig. 2). It has been reported previously that endophilins, SH3 domain-containing lysophosphatidic acid acyltransferases, bind to the proline-rich region of Alix (*21*). Since the endophilin binding region has been mapped to a region encompassing amino acids 748–761 of Alix (*21*) that is distinct from the ABS, the possibility was raised that Alix binds simultaneously to ALG-2 and endophilin in response to Ca^{2+} mobilization. To test this possibility, HEK293 cells were co-transfected with the expression plasmid encoding full-length or deletion mutants of FLAG-tagged Alix (FLAG-Alix, FLAG-AlixΔEBS or FLAG-AlixΔABS; see Fig. 4A) and HA-tagged endophilin I (HA-endophilin I), and the cell lysates were immunoprecipitated with anti-FLAG mAb in the presence of Ca^{2+}. As shown in Fig. 4C lane 1, both endogenous ALG-2 and HA-endophilin I were co-precipitated with FLAG-Alix by anti-FLAG mAb, demonstrating the ability of Alix to associate simultaneously with ALG-2 and endophilin under these conditions. ALG-2 was detected in the immunoprecipitates of FLAG-AlixΔEBS, which lacks the region of amino acids 757–763, but not in these of FLAG-AlixΔABS (lane 2). Conversely, HA-endophilin I was detected in the precipitates of FLAG-AlixΔABS, but not in these of FLAG-AlixΔEBS (lane 3). Neither ALG-2 nor HA-endophilin I was seen in the control precipitates from the lysates of cells transfected with empty vector (lane 4). These results indicate that ALG-2 recognizes a region in Alix distinct from that for endophilin I binding and suggest that Alix interacts simultaneously with ALG-2 and endophilin I in response to Ca^{2+}-signaling.

Requirement of ABS for the Punctate Distribution of AlixCT and Overlapping Localization of ALG-2 with AlixCT—To assess the physiological role of the ABS in Alix in cellular processes, confocal microscopic analysis was performed in HeLa cells transfected with expression plasmids encoding GFP-fused deletion mutant forms of Alix (Fig. 5A). The overexpressed carboxyl-terminal half of Alix fused with GFP (GFP-AlixCT) distributed in a punctate pattern mainly in the perinuclear area (Fig. 5B), which is consistent with a previous report using HEK293 cells (*21*). Endogenous ALG-2 visualized with anti-ALG-2 pAb (*5*, *25*) using goat anti-rabbit IgG-Cy3 as a secondary antibody was detected throughout the cytoplasm, especially in the perinuclear area, and in the nucleoplasm of untransfected cells, whereas a portion of endogenous ALG-2 in GFP-AlixCT expressing cells showed a dot-like pattern co-localizing with the fluorescent foci of GFP-AlixCT (Figs. 5, C and D). Deletion of the EBS from GFP-AlixCT caused scattered distributions of dot-like fluorescent signals, and some ALG-2 co-localized with GFP-AlixCTΔEBS (Figs. 5, E–G). In contrast, the

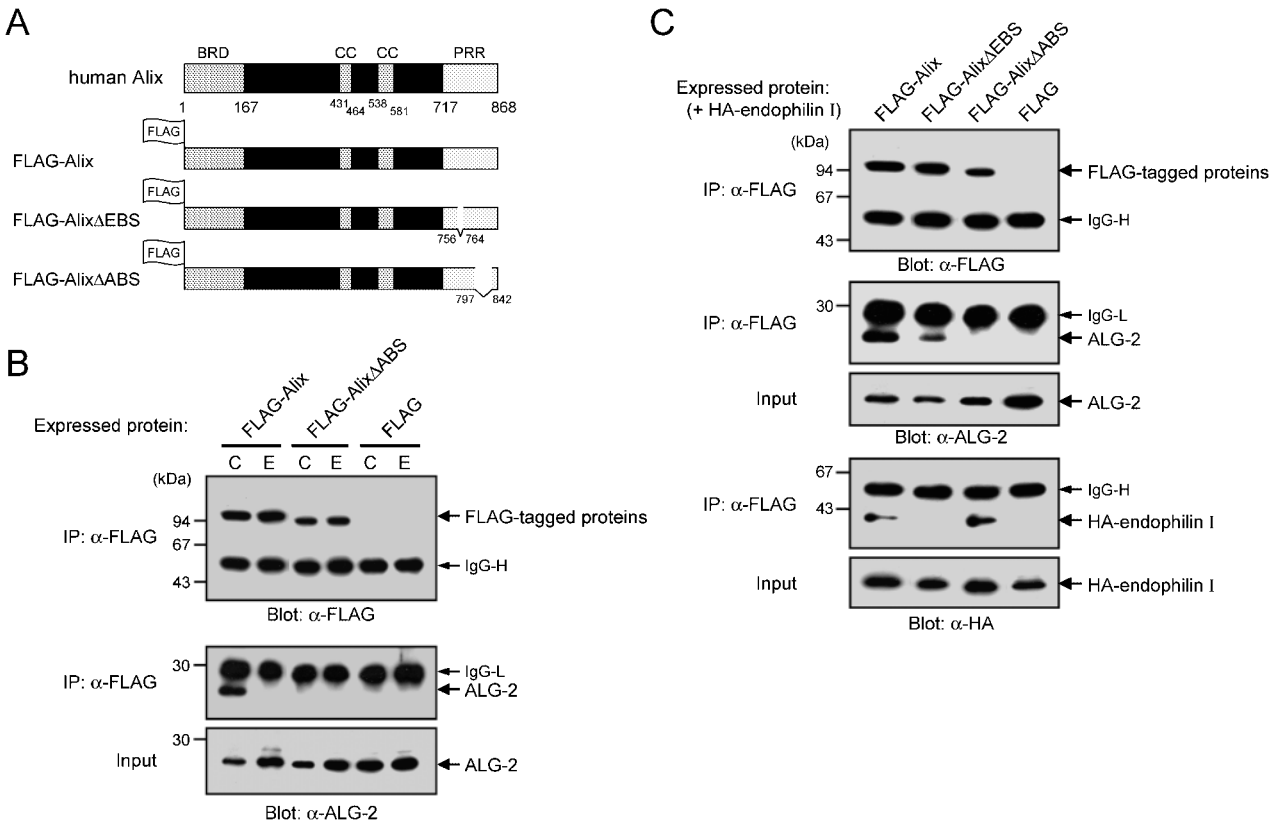

Fig. 4. **The ALG-2 binding sequence (ABS) is required for the interaction of Alix with ALG-2 in mammalian cells.** (A) Schematic representation of FLAG-tagged Alix and Alix deletion constructs. 'BRD', 'CC' and 'PRR' indicate a Bro1-rhophilin-like domain, coiled-coil and proline-rich region, respectively. AlixΔEBS contains a deletion of 8 amino acids (RPPPPVLP) that agree with the endophilin-binding consensus sequence, whereas AlixΔABS is a deletion mutant missing the ALG-2 binding sequence (a.a. 798–841). (B) HEK293 cells transfected with pFLAG-Alix, pFLAG-AlixΔABS or empty vector pCMV-Tag2 were lysed in the presence of 10 μM $CaCl_2$ (*C*) or 5 mM EGTA (*E*) and immunoprecipitated (*IP*) with anti-FLAG mAb. The lysates (*Input*) and immunoprecipitates (*IP*) were analyzed by immunoblotting with anti-FLAG mAb or with anti-ALG-2 pAb. Arrows indicate the positions of each protein. Mouse immunoglobulin heavy chains (*IgG-H*) and light chains (*IgG-L*) were also detected by subsequent immunoblotting. Positions of protein size markers are shown at the left. (C) HEK293 cells co-transfected with pHA-endophilin I and pFLAG-Alix, pFLAG-AlixΔEBS, pFLAG-AlixΔABS or empty vector pCMV-Tag2 were lysed in the presence of 10 μM $CaCl_2$ and immunoprecipitated (*IP*) with anti-FLAG mAb. The lysates (*Input*) and immunoprecipitates (*IP*) were analyzed by immunoblotting with anti-FLAG mAb, anti-ALG-2 pAb or anti-HA mAb. Arrows indicate the positions of each protein. Mouse immunoglobulin heavy chains (*IgG-H*) and light chains (*IgG-L*) were also detected by subsequent immunoblotting. Positions of protein size markers are shown at the left.

removal of the ABS in GFP-AlixCT resulted in a diffuse pattern over the cytoplasm (Fig. 5H) and no difference in the distribution pattern of ALG-2 between untransfected cells and GFP-AlixCTΔABS-expressing cells (Figs. 5, I and J).

Effects of Point Mutations of the PEF Domain in ALG-2 on Its Ca^{2+}-Dependent Interaction with Alix and the Subcellular Localization of ALG-2—ALG-2 possesses two high-affinity Ca^{2+} binding sites at EF1 and EF3 (*26*), and exposes a hydrophobic surface in a Ca^{2+}-dependent manner (*17*, *25*). A double mutation of the glutamic acid residues that provide two oxygen ligands to the Ca^{2+} in both EF-hands completely disrupts the Ca^{2+}-binding capacity of the mutant protein (ALG-$2^{E47A/E114A}$) (*27*). To test the requirement of the Ca^{2+}-binding activity of ALG-2 for the functional interaction with Alix, we first carried out the co-immunoprecipitation experiments using HEK293 cells transfected with the expression plasmids encoding FLAG-tagged ALG-2 (FLAG-ALG-2) or ALG-$2^{E47A/E114A}$ (FLAG-ALG-$2^{E47A/E114A}$) and GFP-Alix or GFP. As shown in Fig. 6A, FLAG-ALG-$2^{E47A/E114A}$ failed to be co-precipitated with GFP-Alix in both presence and absence of Ca^{2+} (lanes 3 and 4), whereas FLAG-ALG-2 was enriched in the precipitates of GFP-Alix in a Ca^{2+}-dependent fashion (lanes 1 and 2). Neither FLAG-ALG-2 nor FLAG-ALG-$2^{E47A/E114A}$ was detected in the precipitates of GFP regardless of the presence or absence of Ca^{2+} (lanes 5–8). These results suggest that the EF1 and EF3 in ALG-2 confer susceptibility to Ca^{2+} for the direct interaction with Alix. We then analyzed HeLa cells overexpressing FLAG-ALG-2 or FLAG-ALG-$2^{E47A/E114A}$ by fluorescence microscopy. FLAG-ALG-2 distributed diffusely in both the cytoplasm and nucleoplasm and concentrated in the juxtanuclear region (Fig. 6B), consistent with the staining pattern of endogenous ALG-2 proteins using our anti-ALG-2 pAb (Fig. 5). A similar distribution was observed with FLAG-ALG-$2^{E47A/E114A}$ except for a decrease in the staining signal near the nucleus (Fig. 6F). Overexpression of GFP-AlixCT induced the accumulation of both FLAG-ALG-2 (Figs. 6C–E) and FLAG-ALG-$2^{E47A/E114A}$ (Figs. 6G–I),

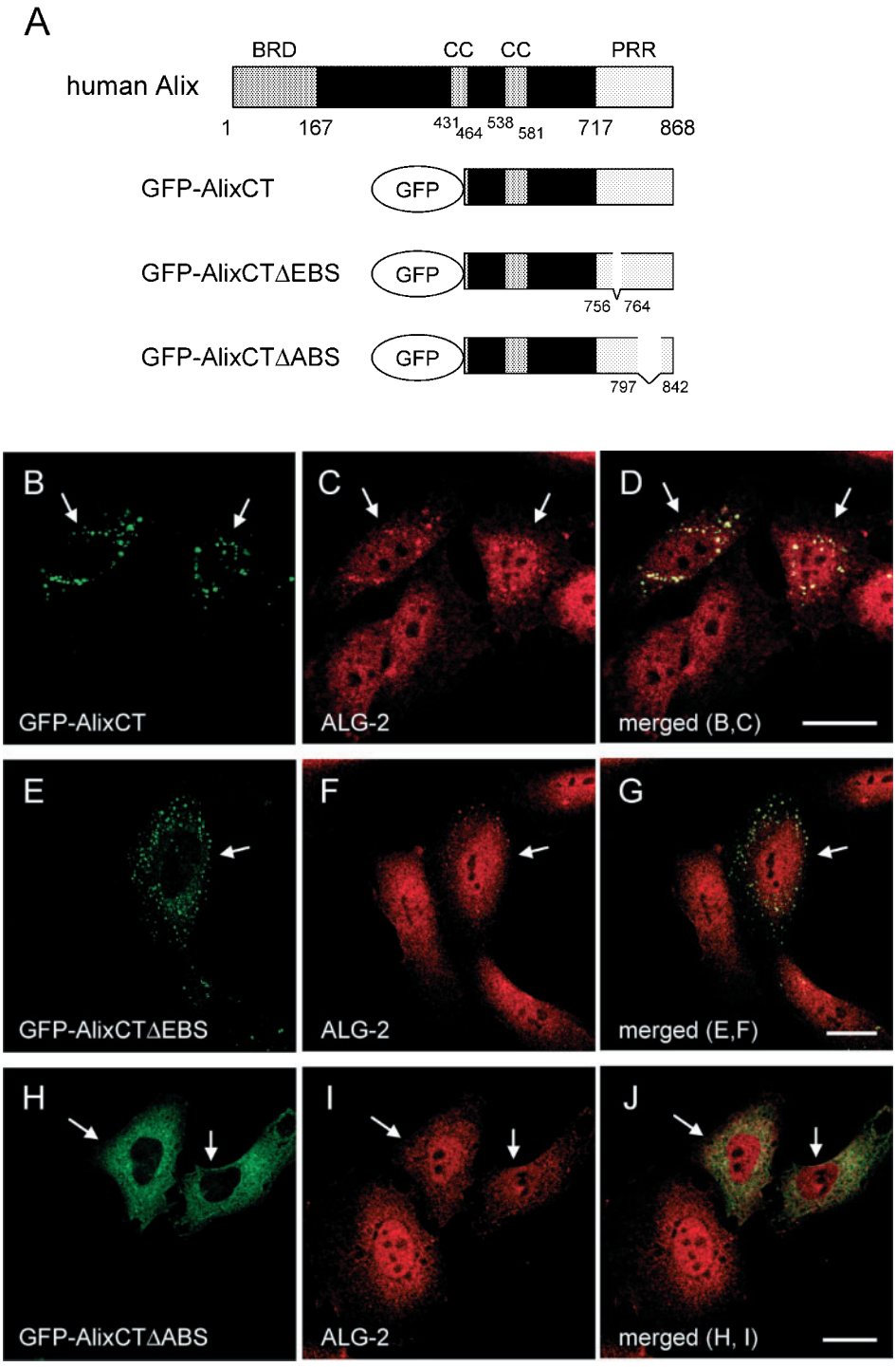

Fig. 5. **Cellular localization of overexpressed mutant forms of Alix and endogenous ALG-2.** (A) Schematic representation of GFP-fused Alix deletion constructs. 'BRD', 'CC' and 'PRR' indicate a Bro1-rhophilin-like domain, coiled-coil and proline-rich region, respectively. AlixCT corresponds to a fragment spanning amino acids 458–868 of Alix. (B–J) HeLa cells transiently transfected with pGFP-AlixCT (B–D), pGFP-AlixCTΔEBS (E–G) or pGFP-AlixΔABS (H–J) constructs were visualized directly (B, E and H; green) or using antibody against ALG-2 (C, F and I; red). Merged images are shown (D, G and J). Arrows indicate cells that expressed GFP-fusion proteins. Bar, 20 μm.

whereas the extent to which FLAG-ALG-2$^{E47A/114A}$ and GFP-AlixCT co-localized varied between transfected cells and tended to be lower than the extent of FLAG-ALG-2 and GFP-AlixCT co-localization.

DISCUSSION

PEF family members have been shown to be involved in regulating a wide variety of Ca^{2+}-induced cellular processes by means of binding to their specific targets (*1*). We are interested in understanding how the complexes between PEF proteins and their target proteins are assembled and how PEF proteins mediate Ca^{2+}-signaling. The experiments described in this report represent a step toward this goal. In this study, two different approaches were undertaken to identify the Alix sequences responsible for the interaction with ALG-2. First, a two-hybrid method was used to map the Alix sequences required for the interaction with ALG-2 (Fig. 1B). The results of this experiment showed that a small domain in the C-terminal proline-rich region of Alix is necessary for the interaction with ALG-2. This domain was mapped to a 28-amino

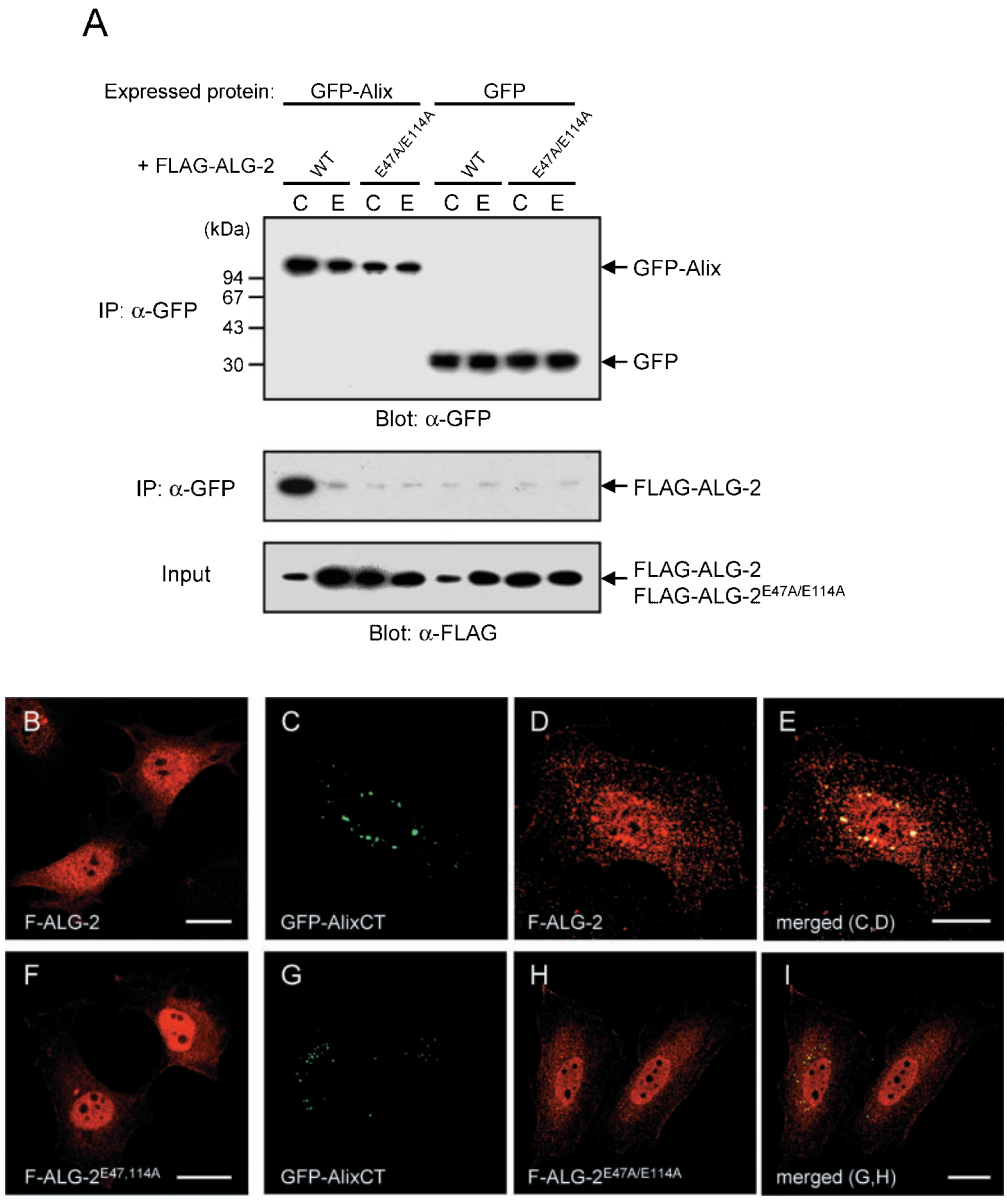

Fig. 6. **Interaction of FLAG-ALG-2 with Alix and its cellular localization in mammalian cells.** (A) HEK293 cells co-transfected with pFLAG-ALG-2 or pFLAG-ALG-2$^{E47A/E114A}$ and pGFP-Alix or empty vector pEGFP-C3 were lysed in the presence of 10 μM $CaCl_2$ (*C*) or 5 mM EGTA (*E*) and immunoprecipitated (*IP*) with anti-GFP pAb. The lysates (*Input*) and immunoprecipitates (*IP*) were analyzed by immunoblotting with anti-GFP mAb or anti-FLAG mAb. Arrows indicate the positions of each protein. Positions of protein size markers are shown at the left. (B–I) HeLa cells transiently transfected with pFLAG-ALG-2 (B), pFLAG-ALG-2$^{E47A/E114A}$ (F), pFLAG-ALG-2, and pEGFP-AlixCT (C–E), or pFLAG-ALG-2$^{E47A/E114A}$ and GFP-AlixCT (G–I) were visualized directly (C and G; green) or using antibody against FLAG (B, D, F, and H; red). Merged images are shown (E and I). Bar, 20 μm.

acid region encompassing residues 796–823. In contrast, the minimal region sufficient for the interaction with ALG-2 in the two-hybrid system was a 52-amino acid region encompassing residues 796–847, 24-amino acid residues longer in the C-terminus. This additional region may play important roles in protein stability or the proper folding of the ALG-2 recognition site in yeast cells. Next, we carried out an overlay assay using bio-ALG-2 as a probe to confirm the results obtained by the two-hybrid experiments and to examine whether ALG-2 interacts directly with Alix. This assay demonstrated that the Ca^{2+}-dependent direct interaction takes place between ALG-2 and a smaller region in Alix that consists of a 33-amino acid region encompassing residues 794–827 (Fig. 3). The amino acid sequence of this region in Alix shows no similarity to the previously identified target sequence for other PEF family proteins, such as the PEST domain of IκBα, which is one of the targets for the PEF domain of the calpain large subunit (*28*), the large hydrophobic loop region of presenilin 2, which is another target for the PEF domain of both calpain large subunit (*29*) and sorcin (*30*), or regions A and C of the functional inhibitory domain of calpastatin, which bind to domain IV (PEF domain in the large subunit) and domain VI (PEF

domain in the small subunit) of calpain, respectively (*31*, *32*). Thus, the region comprising amino acids 798–827 in Alix may define novel binding motif for the Ca^{2+}-binding form of PEF domains, and interact specifically with ALG-2. Indeed, our two-hybrid system could not detect an interaction signal between Alix and other PEF family proteins, such as the calpain small subunit, peflin and sorcin (data not shown). The amino-terminal regions of annexin VII and annexin XI, which are also targets for ALG-2 (*17*, *33*), exhibit partial homology to the ABS in Alix, and similar biased amino acid compositions are found in their sequences, which are rich in Pro, Tyr, and Gly (the ABS in Alix: Pro, 30.3%; Tyr, 21.2%; Gly, 15.2%; annexin VII residues 1–145: Pro, 28.3%; Tyr, 11.0%; Gly, 25.5%; annexin XI residues 1–176: Pro, 31.8%; Tyr, 9.1%; Gly, 18.2%). In the crystal structure of the Ca^{2+}-loaded ALG-2 dimer treated with elastase, the Pro/Gly-rich hydrophobic decapeptide, presumably originating from N-terminal extensions of ALG-2, binds at a largely hydrophobic cleft formed between the helix α7 and the loop connecting EF3 and EF4 in the PEF domain (*26*). The ABS in Alix, as well as the N-terminal Pro/Gly/Tyr-rich regions of annexin VII and annexin XI, may bind to ALG-2 in a way that resembles the occupation of the exposed hydrophobic surface in the PEF domain of ALG-2 by the N-terminal hydrophobic ALG-2 segments. Since the ALG-2 dimer has two hydrophobic areas derived from each PEF domain of the subunit molecule, this dimer could function as a Ca^{2+}-dependent adaptor by recruiting two distinct target molecules. It is also possible that the ALG-2-binding peptides promote the conformational rearrangement that introduces a significant change in the shape of the dimer and exposes the hydrophobic N-terminal region of ALG-2 in a coordinated manner with Ca^{2+}, which leads to translocation of the ALG-2 complex to the membrane. Results of future structural analyses on the complex between ALG-2 and the ALG-2 binding region in Alix should clarify the binding mode and exact role of this interaction.

The sequence of the ALG-2 binding region in Alix has a strikingly repetitive character, $(PxY)_4$, in its central region (Fig. 3A). Several mutations provide insights regarding amino acids that are crucial for the fundamental properties of the interaction with ALG-2. Through alanine substitutions and *in vitro* overlay studies, it was determined that the four prolines in $(PxY)_4$ play important roles in this interaction. Moreover, the four tyrosines are also required for binding to ALG-2 (Fig. 3B). Assuming this tandem repeat adopts the left-handed polyproline II (PPII) helical structure that is an extended structure with three residue per turn (*34*, *35*), the importance of these residues in $(PxY)_4$ observed herein could be explained by their position in the PPII helix. Accordingly, prolines would be essential for proper formation of this repeat and/or function in binding to ALG-2 in a way that resembles the binding of SH3 domains to their proline-rich target motifs. The adjacent tyrosines would also be part of the surface of the PPII helix that contacts the recognition pocket of ALG-2 molecule. The tyrosine hydroxyl group is hydrophilic and polar, so readily participates in hydrogen bonding, and can potentially undergo regulatory phosphorylation. Mutations of four tyrosines in the PxY repeats to nonpolar aromatic residues, phenylalanines, also extinguished ALG-2 binding activity. Thus, these tyrosine residues are critical components of $(PxY)_4$ in the ALG-2 binding region. While the $(PxY)_4$ is a crucial element for the direct binding to ALG-2, it was not sufficient for stable complex formation in our two-hybrid system (Fig. 1B). Through the creation of truncated versions of the proline-rich region in Alix, we found that the sequence following the PxY repeats is also necessary for binding to ALG-2 in an overlay assay. By performing mutational analysis, we further determined that three prolines, not three tyrosines, in this C-terminal extension are important for stable binding of Alix to ALG-2 (Fig. 3B). It is likely that this region may also form a PPII helix that places the relevant side chains in the appropriate conformation. Recently, ALG-2 was reported to interact with the death domain of Fas in a Ca^{2+}-dependent fashion (*36*). However, the commercially available mAb against ALG-2 utilized in the experiment has been criticized for its specificity to endogenous ALG-2 (*37*). So, it remains unclear whether ALG-2 interacts functionally *in vivo* with the death domain of Fas, which has no sequence similarity with the ALG-2 binding region in Alix.

It has been reported that the C-terminal region of Alix functions as the binding surface for several proteins, including endophilins (*21*) and glioma-associated protein SETA (*38*), which is an isoform of CIN85/Ruk (*39*, *40*). Each endophilin isoform possesses an SH3 domain at its C-terminus that binds to the proline-rich region in Alix, while the longest form of SETA/CIN85/Ruk encodes three SH3 domains at its N-terminus, each of which appears to show a different binding specificity for the putative CIN85-binding site in Alix. The endophilin-binding site has been mapped to residues 748–761 in Alix, which contains a PxRPPPP consensus sequence for endophilins (*21*), whereas no interaction was detected between ALG-2 and the region in Alix containing this sequences in our two-hybrid system (Fig. 1B). Further, co-immunoprecipitation experiments using deletion mutants of Alix indicated that the required region in Alix for the interaction with ALG-2 was distinct from that for the interaction with endophilin I in mammalian cells: ALG-2 on residues 798–841, endophilin I on residues 757–763 (Fig. 4C). Since ALG-2 and endophilin I appeared to bind simultaneously to Alix in the presence of Ca^{2+} (Fig. 4C), it is possible that the Ca^{2+}-dependent interaction of ALG-2 with Alix affects the localization of this complex and/or the enzymatic activity of endophilins that leads to the modulation of membrane curvature under physiological conditions. Our recently obtained data indicates that the CIN85-binding region in Alix is located at a site different from the binding sites for ALG-2 and endophilins (Shibata *et al.*, manuscript in preparation). Although it remains unclear whether the Ca^{2+}-dependent interaction of ALG-2 with Alix leads to a conformational change of Alix that affects the dissociation or association of other binding factors, the proline-rich region at the C-terminus of Alix may provide a platform for the assembly of these proteins and ALG-2 could serve as the mediator of Ca^{2+} signaling to this complex through direct interaction with Alix.

Chatellard-Causse al. reported that the overexpression of AlixCT leads to an accumulation of perinuclear tubulovesicular structures, which are transformed into a few

very large vacuoles upon co-expression with endophilins (*21*). In this study, we demonstrated that the ALG-2-binding sequence (ABS) in AlixCT, but not the endophilin-binding sequence (EBS), is required for the punctate distribution of GFP-AlixCT (Fig. 5). The interaction of ALG-2 with Alix may be a critical step in the translocation of these proteins to biological membranes, where recruited endophilins modulate membrane shape. Furthermore, the overexpression of AlixCT induced the punctate distribution of endogenous and FLAG-tagged ALG-2, which overlaps the AlixCT-location (Figs. 5 and 6). Although it remains unclear to which types of intracellular compartment AlixCT localizes, the co-localization of ALG-2 to overexpressed AlixCT under physiological conditions suggests that Ca^{2+} is relatively rich in the surrounding area of the compartments that AlixCT and ALG-2 are co-located. The distribution of several endosomal marker proteins, including EEA1 (early endosome) and Lamp-1 (late endosome), did not co-localize with that of GFP-AlixCT and did not differ significantly between untransfected cells and GFP-AlixCT-transfected cells, whereas the fluorescent foci of GFP-AlixCT partially overlaps with that of $SKD1^{E235Q}$ compartment, an aberrant compartment derived from an endosomal pathway (*41*, *42*), in co-expressed cells (data not shown). Taken together with the observations that endosomes are one of the Ca^{2+} stores in cells, and that the lumenal Ca^{2+} in endosomes is required for its acidification (*43*) and the homo- and hetero-typic fusion of endocytic compartment (*44*, *45*), it is possible that ALG-2 may function as a Ca^{2+} sensor at the space near these endosomes and the complex between ALG-2 and Alix translocates to endosomal membrane. Recently, Alix has been identified as a host protein that links the $p6^{Gag}$ protein of human immunodeficiency virus-1 (HIV-1) and the $p9^{Gag}$ of equine infectious anemia virus (EIAV) to the late endosomal sorting complex essential for virus budding (*46*, *47*). Since the overexpression of an Alix mutant that lacks the C-terminal proline-rich region containing the ALG-2 binding site inhibits HIV-1 budding at a late stage (*46*), ALG-2 may function to modulate the activity of Alix in virus budding.

We speculate that the Ca^{2+}-binding deficient form of ALG-2, $ALG\text{-}2^{E47A/114A}$ (*27*), acts as dominant negative ALG-2 in cells, but the accumulation of GFP-AlixCT does not completely disappear in most cells co-expressing $ALG\text{-}2^{E47A/114A}$ and GFP-AlixCT (Fig. 6). The expression level of $ALG\text{-}2^{E47A/114A}$ may not be sufficient for the blockage of the function of endogenous proteins or the hetrodimer between the wild type, and the mutant form of ALG-2 could be a fully functional complex for the response to Ca^{2+} and the anchor of AlixCT. Further studies on ALG-2 and Alix in the light of membrane trafficking using knockout or knockdown techniques may provide new insights into the role of Ca^{2+} in vesicle transport and virus budding.

This work was supported by a Grant-in-Aid for Scientific Research B (to M.M.) and a Grant-in-Aid for Young Scientists B (to H.S.). We thank Dr. K. Hitomi in our laboratory for valuable discussions.

REFERENCES

1. Maki, M., Kitaura, Y., Satoh, H., Ohkouchi, S., and Shibata, H. (2002) Structures, functions and molecular evolution of the penta-EF-hand Ca^{2+}-binding proteins. *Biochim. Biophys. Acta* **1600**, 51–60
2. Blanchard, H., Grochulski, P., Li, Y., Arthur, J.S., Davies, P.L., Elce, J.S., and Cygler, M. (1997) Structure of a calpain Ca^{2+}-binding domain reveals a novel EF-hand and Ca^{2+}-induced conformational changes. *Nat. Struct. Biol.* **4**, 532–538
3. Lin, G.D., Chattopadhyay, D., Maki, M., Wang, K.K., Carson, M., Jin, L., Yuen, P.W., Takano, E., Hatanaka, M., DeLucas, L.J., and Narayana, S.V. (1997) Crystal structure of calcium bound domain VI of calpain at 1.9 Å resolution and its role in enzyme assembly, regulation, and inhibitor binding. *Nat. Struct. Biol.* **4**, 539–547
4. Maki, M., Narayana, S.V., and Hitomi, K. (1997) A growing family of the Ca^{2+}-binding proteins with five EF-hand motifs. *Biochem. J.* **328** (Pt 2), 718–720
5. Kitaura, Y., Matsumoto, S., Satoh, H., Hitomi, K., and Maki, M. (2001) Peflin and ALG-2, members of the penta-EF-hand protein family, form a heterodimer that dissociates in a Ca^{2+}-dependent manner. *J. Biol. Chem.* **276**, 14053–14058
6. Kitaura, Y., Satoh, H., Takahashi, H., Shibata, H., and Maki, M. (2002) Both ALG-2 and peflin, penta-EF-hand (PEF) proteins, are stabilized by dimerization through their fifth EF-hand regions. *Arch. Biochem. Biophys.* **399**, 12–18
7. Yoshizawa, T., Sorimachi, H., Tomioka, S., Ishiura, S., and Suzuki, K. (1995) A catalytic subunit of calpain possesses full proteolytic activity. *FEBS Lett.* **358**, 101–103
8. Elce, J.S., Davies, P.L., Hegadorn, C., Maurice, D.H., and Arthur, J.S. (1997) The effects of truncations of the small subunit on m-calpain activity and heterodimer formation. *Biochem. J.* **326** (Pt 1), 31–38
9. Hansen, C., Tarabykina, S., la Cour, J.M., Lollike, K., and Berchtold, M.W. (2003) The PEF family proteins sorcin and grancalcin interact *in vivo* and *in vitro*. *FEBS Lett.* **545**, 151–154
10. Vito, P., Lacana, E., and D'Adamio, L. (1996) Interfering with apoptosis: Ca^{2+}-binding protein ALG-2 and Alzheimer's disease gene ALG-3. *Science* **271**, 521–525
11. Lacana, E., Ganjei, J.K., Vito, P., and D'Adamio, L. (1997) Dissociation of apoptosis and activation of IL-1β-converting enzyme/Ced-3 proteases by ALG-2 and the truncated Alzheimer's gene ALG-3. *J. Immunol.* **158**, 5129–5135
12. Jang, I.K., Hu, R., Lacana, E., D'Adamio, L., and Gu, H. (2002) Apoptosis-linked gene 2-deficient mice exhibit normal T-cell development and function. *Mol. Cell. Biol.* **22**, 4094–4100
13. Ohkouchi, S., Nishio, K., Maeda, M., Hitomi, K., Adachi, H., and Maki, M. (2001) Identification and characterization of two penta-EF-hand Ca^{2+}-binding proteins in *Dictyostelium discoideum*. *J. Biochem.* **130**, 207–215
14. Aubry, L., Mattei, S., Blot, B., Sadoul, R., Satre, M., and Klein, G. (2002) Biochemical characterization of two analogues of the apoptosis-linked gene 2 protein in *Dictyostelium discoideum* and interaction with a physiological partner in mammals, murine Alix. *J. Biol. Chem.* **277**, 21947–21954
15. Missotten, M., Nichols, A., Rieger, K., and Sadoul, R. (1999) Alix, a novel mouse protein undergoing calcium-dependent interaction with the apoptosis-linked-gene 2 (ALG-2) protein. *Cell Death. Differ.* **6**, 124–129
16. Vito, P., Pellegrini, L., Guiet, C., and D'Adamio, L. (1999) Cloning of AIP1, a novel protein that associates with the apoptosis-linked gene ALG-2 in a Ca^{2+}-dependent reaction. *J. Biol. Chem.* **274**, 1533–1540
17. Satoh, H., Shibata, H., Nakano, Y., Kitaura, Y., and Maki, M. (2002) ALG-2 interacts with the amino-terminal domain of annexin XI in a Ca^{2+}-dependent manner. *Biochem. Biophys. Res. Commun.* **291**, 1166–1172
18. Che, S., El Hodiri, H.M., Wu, C.F., Nelman-Gonzalez, M., Weil, M.M., Etkin, L.D., Clark, R.B., and Kuang, J. (1999) Identification and cloning of Xp95, a putative signal transduction protein in *Xenopus* oocytes. *J. Biol. Chem.* **274**, 5522–5531

19. Wu, Y., Pan, S., Che, S., He, G., Nelman-Gonzalez, M., Weil, M.M., and Kuang, J. (2001) Overexpression of Hp95 induces G1 phase arrest in confluent HeLa cells. *Differentiation* **67**, 139–153
20. Wu, Y., Pan, S., Luo, W., Lin, S.H., and Kuang, J. (2002) Hp95 promotes anoikis and inhibits tumorigenicity of HeLa cells. *Oncogene* **21**, 6801–6808
21. Chatellard-Causse, C., Blot, B., Cristina, N., Torch, S., Missotten, M., and Sadoul, R. (2002) Alix (ALG-2-interacting protein X), a protein involved in apoptosis, binds to endophilins and induces cytoplasmic vacuolization. *J. Biol. Chem.* **277**, 29108–29115
22. Schmidt, A., Wolde, M., Thiele, C., Fest, W., Kratzin, H., Podtelejnikov, A.V., Witke, W., Huttner, W.B., and Soling, H.D. (1999) Endophilin I mediates synaptic vesicle formation by transfer of arachidonate to lysophosphatidic acid. *Nature* **401**, 133–141
23. Katoh, K., Shibata, H., Suzuki, H., Nara, A., Ishidoh, K., Kominami, E., Yoshimori, T., and Maki, M. (2003) The ALG-2-interacting protein Alix associates with CHMP4b, a human homologue of yeast Snf7 that is involved in multivesicular body sorting. *J. Biol. Chem.* **278**, 39104–39113
24. Hitomi, K., Yokoyama, A., and Maki, M. (1998) Expression of biologically active human calpastatin in baculovirus-infected insect cells and in *Escherichia coli*. *Biosci. Biotechnol. Biochem.* **62**, 136–141
25. Maki, M., Yamaguchi, K., Kitaura, Y., Satoh, H., and Hitomi, K. (1998) Calcium-induced exposure of a hydrophobic surface of mouse ALG-2, which is a member of the penta-EF-hand protein family. *J. Biochem.* **124**, 1170–1177
26. Jia, J., Tarabykina, S., Hansen, C., Berchtold, M., and Cygler, M. (2001) Structure of apoptosis-linked protein ALG-2: insights into Ca^{2+}-induced changes in penta-EF-hand proteins. *Structure* **9**, 267–275
27. Lo, K.W., Zhang, Q., Li, M., and Zhang, M. (1999) Apoptosis-linked gene product ALG-2 is a new member of the calpain small subunit subfamily of Ca^{2+}-binding proteins. *Biochemistry* **38**, 7498–7508
28. Shumway, S.D., Maki, M., and Miyamoto, S. (1999) The PEST domain of IκBα is necessary and sufficient for *in vitro* degradation by μ-calpain. *J. Biol. Chem.* **274**, 30874–30881
29. Shinozaki, K., Maruyama, K., Kume, H., Tomita, T., Saido, T.C., Iwatsubo, T., and Obata, K. (1998) The presenilin 2 loop domain interacts with the μ-calpain C-terminal region. *Int. J. Mol. Med.* **1**, 797–799
30. Pack-Chung, E., Meyers, M.B., Pettingell, W.P., Moir, R.D., Brownawell, A.M., Cheng, I., Tanzi, R.E., and Kim, T.W. (2000) Presenilin 2 interacts with sorcin, a modulator of the ryanodine receptor. *J. Biol. Chem.* **275**, 14440–14445
31. Yang, H.Q., Ma, H., Takano, E., Hatanaka, M., and Maki, M. (1994) Analysis of calcium-dependent interaction between amino-terminal conserved region of calpastatin functional domain and calmodulin-like domain of μ-calpain large subunit. *J. Biol. Chem.* **269**, 18977–18984
32. Takano, E., Ma, H., Yang, H.Q., Maki, M., and Hatanaka, M. (1995) Preference of calcium-dependent interactions between calmodulin-like domains of calpain and calpastatin subdomains. *FEBS Lett.* **362**, 93–97
33. Satoh, H., Nakano, Y., Shibata, H., and Maki, M. (2002) The penta-EF-hand domain of ALG-2 interacts with amino-terminal domains of both annexin VII and annexin XI in a Ca^{2+}-dependent manner. *Biochim. Biophys. Acta* **1600**, 61–67
34. Williamson, M.P. (1994) The structure and function of proline-rich regions in proteins. *Biochem. J.* **297** (Pt 2), 249–260
35. Kay, B.K., Williamson, M.P., and Sudol, M. (2000) The importance of being proline: the interaction of proline-rich motifs in signaling proteins with their cognate domains. *FASEB J.* **14**, 231–241
36. Jung, Y.S., Kim, K.S., Kim, K.D., Lim, J.S., Kim, J.W., and Kim, E. (2001) Apoptosis-linked gene 2 binds to the death domain of Fas and dissociates from Fas during Fas-mediated apoptosis in Jurkat cells. *Biochem. Biophys. Res. Commun.* **288**, 420–426
37. la Cour, J.M., Mollerup, J., Winding, P., Tarabykina, S., Sehested, M., and Berchtold, M.W. (2003) Up-regulation of ALG-2 in hepatomas and lung cancer tissue. *Amer. J. Pathol.* **163**, 81–89
38. Chen, B., Borinstein, S.C., Gillis, J., Sykes, V.W., and Bogler, O. (2000) The glioma-associated protein SETA interacts with AIP1/Alix and ALG-2 and modulates apoptosis in astrocytes. *J. Biol. Chem.* **275**, 19275–19281
39. Take, H., Watanabe, S., Takeda, K., Yu, Z.X., Iwata, N., and Kajigaya, S. (2000) Cloning and characterization of a novel adaptor protein, CIN85, that interacts with c-Cbl. *Biochem. Biophys. Res. Commun.* **268**, 321–328
40. Gout, I., Middleton, G., Adu, J., Ninkina, N.N., Drobot, L.B., Filonenko, V., Matsuka, G., Davies, A.M., Waterfield, M., and Buchman, V.L. (2000) Negative regulation of PI 3-kinase by Ruk, a novel adaptor protein. *EMBO J.* **19**, 4015–4025
41. Yoshimori, T., Yamagata, F., Yamamoto, A., Mizushima, N., Kabeya, Y., Nara, A., Miwako, I., Ohashi, M., Ohsumi, M., and Ohsumi, Y. (2000) The mouse SKD1, a homologue of yeast Vps4p, is required for normal endosomal trafficking and morphology in mammalian cells. *Mol. Biol. Cell* **11**, 747–763
42. Bishop, N. and Woodman, P. (2000) ATPase-defective mammalian VPS4 localizes to aberrant endosomes and impairs cholesterol trafficking. *Mol. Biol. Cell* **11**, 227–239
43. Gerasimenko, J.V., Tepikin, A.V., Petersen, O.H., and Gerasimenko, O.V. (1998) Calcium uptake via endocytosis with rapid release from acidifying endosomes. *Curr. Biol.* **8**, 1335–1338
44. Holroyd, C., Kistner, U., Annaert, W., and Jahn, R. (1999) Fusion of endosomes involved in synaptic vesicle recycling. *Mol. Biol. Cell* **10**, 3035–3044
45. Pryor, P.R., Mullock, B.M., Bright, N.A., Gray, S.R., and Luzio, J.P. (2000) The role of intraorganellar Ca^{2+} in late endosome-lysosome heterotypic fusion and in the reformation of lysosomes from hybrid organelles. *J. Cell Biol.* **149**, 1053–1062
46. Strack, B., Calistri, A., Craig, S., Popova, E., and Göttlinger, H.G. (2003) AIP1/ALIX is a binding partner for HIV-1 p6 and EIAV p9 functioning in virus budding. *Cell* **114**, 689–699
47. von Schwedler, U.K., Stuchell, M., Müller, B., Ward, D.M., Chung, H.Y., Morita, E., Wang, H.E., Davis, T., He, G.P., Cimbora, D.M., Scott, A., Kräusslich, H.G., Kaplan, J., Morham, S.G., and Sundquist, W.I. (2003) The protein network of HIV budding. *Cell* **114**, 701–713